

DAMAGE MECHANISMS AND FRACTURE BEHAVIOUR OF THERMALLY-AGED DUPLEX STAINLESS STEEL : MODELLING OF THE FRACTURE TOUGHNESS USING LOCAL APPROACH

P. Lamagnère¹, A. Hazarabedian¹, D. Guérin¹, J. Reuchet², B. Marini¹

¹CEA Saclay, DTA-CEREM, 91191 Gif-sur-Yvette Cedex - France

²IPSN, DES-SAMS, BP6, 92265 Fontenay-aux-Roses Cedex - France

ABSTRACT

The damage mechanisms and fracture behaviour of two duplex stainless steels have been studied after thermal ageing at 325°C during 30000 hours. The ferrite phase fractures by cleavage whereas austenite lathes remain ductile. The heterogeneous nucleation rate of cleavage cracks with strain has been characterised using Voronoï cells analysis from surface replicas extracted during tensile test.

The observed damage mechanism and fracture behaviour are well described by a model of local approach of fracture. The model has been applied to notched tensile specimens using 2D axisymmetric FE calculations with Castem2000 software developed at CEA. A good prediction of the data scattering and size effect on the mean strain at failure has been obtained. Finally, 2D calculations have been made to simulate crack propagation in CT specimens tested at room temperature. The simulated J_{1c} and crack propagation resistance are in agreement with experimental data.

INTRODUCTION

Cast duplex stainless steels with austenite ferrite microstructure are used in Pressurised Water Reactors in the primary loop of the cooling system. Long time exposure at service temperature, namely between 280 and 320°C, results in a significant decrease of ductility and fracture toughness known as the " 475°C embrittlement " [1]. This phenomenon is related to the precipitation hardening of ferrite phase [2] occurring mainly by decomposition of ferrite in iron-rich α and chromium-rich α' domains.

Due to the coarse microstructure of austenitic and ferritic phases, the fracture properties of aged duplex steels determined with laboratory specimens are strongly dispersed [3]. This microstructure also induces a size effect in the experimental results and raises the problem of transferability of toughness properties from laboratory specimens to structures.

The first goal of this work is to study the damage mechanisms and fracture behaviour of two duplex stainless steels after thermal ageing at 325°C. It will be known that the observations are in agreement with the hypothesis of the model of fracture toughness developed by P. Joly and L. Devillers-Guerville et al. [4,5]. Therefore, this local approach of failure is used to predict the scatter and size effects of toughness properties.

MATERIALS, THERMAL TREATMENTS AND EXPERIMENTS

The materials used in this study are two duplex stainless steels of CF8M grade with ferrite content and composition as presented in Table 1. These materials were prepared by casting in sand mould present a complex interconnected microstructure of ferrite and austenite laths about 20 μ m thick (see Figure 1). The typical ferrite grain size is 1 mm and each ferrite grain contains about 3 austenite grains. The crystallographic orientations of the ferrite grains are almost randomly distributed.

The specimens were aged at 325°C up to 30000 hours. We have analysed the fracture behaviour after ageing through macroscopic and fractographic examinations. Metallographic investigations of the damage mechanisms have also been made.

In addition, notched tensile specimens of various minimum radius (3.5, 6 and 10 mm) and notch radius were used to characterise the size effect on failure properties and its scattering at room temperature. The fracture toughness was also determined using compact tensile specimens at room temperature (CTJ20).

TABLE 1
COMPOSITION AND FERRITE CONTENT OF THE DUPLEX STAINLESS STEELS

Material	C	Cr	Ni	Mo	Mn	Si	Cu	N2 (ppm)	Ferrite content
258	0.033	22.28	9.92	2.34	0.91	0.86	0.26	510	32%
259	0.023	20.48	10.01	2.50	0.87	0.90	0.22	530	20%

FRACTURE BEHAVIOUR

As ferritic phase hardens with ageing, the macroscopic appearance of fracture in tension changes from a complete ductile to a mixed brittle-ductile mode. After ageing at 325°C for 30000 hours, fractographic examinations reveal that the ferrite phase fractures in a brittle mode while austenite remains ductile (see Figure 2). At room temperature, brittle failure of ferrite occurs mainly by cleavage while shear cracks are also observed on 20% ferrite steel (steel 259). The final fracture occurs with the ductile rupture of the austenite lathes located between the cleavage cracks (see Figure 3). As indicated by P. Joly [4], failure is induced by the continuous nucleation of cleavage cracks in ferrite during the tensile stage. Metallographic observations have shown that cleavage cracks in ferrite are heterogeneously distributed in clusters of size about the austenite grain size. The nucleation rate of cleavage cracks with strain is strongly dispersed from one cluster to another. We have reported in Figure 4 the crack densities observed in steel 258 as a function of strain. These results have been obtained using Voronoï cells analysis [6] from surface replicas extracted at various stages of a tensile test.

We have characterised the scattering of the failure properties using notched round tensile specimens. As already mentioned by S. Carassou et al. [7], the experimental scatter results in a size effect corresponding to a decrease of the mean strain at failure when the specimen size is increased (see Figure 5a and b for steels 258 and 259, resp.). In addition, fracture toughness experiments were performed at room temperature using CTJ20 specimens with 20% side grooves. The crack initiation was detected by potential drop method and crack growth was measured post-mortem. The results reported in Figure 6 for steel 258 show a large scatter in the fracture toughness and crack propagation resistance. J_{1c} varies from 24 to 53 kJ/m² for steel 258 (30% ferrite) and from 83 to 153 kJ/m² for steel 259 (20% ferrite). However a stable crack growth is obtained which we ascribe to the ductile behaviour of the austenitic phase.

MODELLING OF THE FRACTURE TOUGHNESS

The data scattering and size effect are related to the coarse microstructure of duplex steels and to the heterogeneous distribution of cleavage cracks described above. The observed damage mechanism and fracture behaviour are well described by the model of local approach of fracture, first introduced by P. Joly [4]. In this model, the cleavage cracks induce a material softening described by the Gurson Tvergaard Needleman (GTN) plastic flow potential [8]. The nucleation part of the porosity, f_n , is related to the continuous nucleation of cleavage cracks in ferrite :

$$\dot{f}_n = A_n \cdot \dot{\varepsilon}_p$$

where ε_p is the plastic strain and A_n is the cleavage cracks nucleation rate. The relations for porosity evolution have been modified from the GTN model since cleavage cracks do not induce any volume variation [5].

We are taking into account the distribution of cracks in clusters by introducing a statistical distribution of nucleation rates in the material. This is done by dividing the modelled specimen into cubes of the mean clusters size. Then, a uniform nucleation rate, A_n , derived from the distribution of nucleation rates in the clusters is affected to each cube using a von Neumann method [9]. The parameters of the distribution are :

- the mean volume of clusters, V_0 , determined from metallographic examinations,
- the surface ratio of clusters, S_a ,
- the maximum nucleation rate in the clusters, A_{sup} ,
- the homogeneous nucleation rate outside of a cluster, A_{inf} .

The nucleation rate in the clusters is assumed to be uniformly distributed between A_{inf} and A_{sup} . S_a , A_{sup} and A_{inf} have been adjusted to fit the experimental results of tensile tests on notched specimens AE2-3.5 (diameter 3.5mm and notch radius 2x3.5/10mm). The parameters values presented in Table 2 (data from AE2-3.5 specimens) are in reasonable agreement with the experimental values (see Figure 4).

Finally, the voids coalescence occurs when a critical porosity, f_c , is reached. f_c has been determined as the porosity leading to plastic localisation on specimens AE2-3.5. We assume that localisation is reached at the maximum of the local von Mises stress : $\frac{\partial \sigma_{eq}}{\partial \varepsilon_{eq}} = 0$, leading to a critical porosity $f_c = 7\%$ for steel 258.

TABLE 2
PARAMETERS OF THE NUMERICAL SIMULATION

Parameters	V_0 μm^3	S_a	A_{sup}	A_{inf}	f_c %
258	$(300)^3$	0.03	0.62	0.015	7

In a first step, the model has been applied to notched tensile specimens using 2D axisymmetric FE calculation with Castem2000 software developed at CEA. In that case, due to the low value of nucleation rate, the softening effect of cleavage cracks can be neglected. The results are plotted in Figure 5a and b for steels 258 and 259, resp., with comparison to experimental data. We can note that the model provide a good prediction of the data scattering and size effect on the mean strain at failure. However, in the case of steel 258 the effect of notch radius is not described correctly due to the heterogeneous microstructure of the steel.

Fractographic observations have shown that the ferrite grain size was smaller for AE10 specimens than for AE2 ones.

Finally the model has been applied to simulate crack propagation in CT specimens tested at room temperature in the case of steel 258 aged during 30000 hours at 325°C. 2D calculations have been made with various distributed nucleation rates derived from the parameters values presented in Table 2 (data from AE2-3.5 specimens). Simulated clusters in 2D calculations are square beams, therefore, the higher nucleation rate found in the 52 volume elements located over the full thickness of the specimen is considered. Thus the predicted toughness will represent a lower bound of the experimental toughness. A mesh size of 100µm, corresponding to the mean size of a single ferrite and austenite lath, has been chosen in the crack tip area. According to L. Devillers-Guerville recommendations [5], square elements with 8 nodes and 4 integration points have been used. In Figure 7a we present a 2D CT specimen with a colour scale showing the simulated nucleation rates around the crack tip.

The results plotted in Figure 6 are in good agreement with the experimental data. The simulated J_{1c} varies from 21 to 45 kJ/m² and the simulated crack propagation resistance is realistic. A focus on the crack tip presented in Figure 7b shows that the tortuous experimental crack path in duplex steels can be described by the model. The change in the crack plane is directly related to the distributed nucleation rate in the material.

CONCLUSION

The effects of thermal ageing at 325°C on the damage mechanism and fracture behaviour of two duplex stainless steels (resp. 20 and 32% ferrite) have been studied. Ferrite hardening during ageing results in a change from ductile to mixed brittle-ductile fracture behaviour associated with a loss of ductility. After ageing, fracture is mainly nucleated by cleavage cracks of ferrite lathes. Macroscopic cracks result from the coalescence of brittle cracks in ferrite by ductile fracture of the surrounding austenite lathes.

The scattering and size effect of the fracture properties of aged duplex steels have been studied by tensile tests at room temperature on notched round specimens. These tests characterise the loss of ductility when specimen size increases. The scattering of failure properties is related to the coarse microstructure of duplex stainless steel and to the heterogeneous distribution of the cleavage cracks of ferrite.

A model based on local approach of failure, developed by P. Joly et al., has been applied to the materials of the study. The scattering and size effect of the fracture properties are correctly described as far as the material microstructure is constant all over the product. Moreover, the model provides a good prediction of the fracture toughness measured on compact tension specimens. Further work including 3D calculations and simulations of large stable propagations are planned in order to complete the evaluation the transferability of toughness properties from laboratory specimens to structures.

ACKNOWLEDGEMENTS

The authors are grateful to the Institut de Protection et Sureté Nucléaire (IPSN/SAMS) for their financial support. We would like to thank Dr. T. Charras from CEA/SEMT and Dr. P. Forget from CEA/CEREM for their help on numerical simulation.

REFERENCES

1. Chung, H.M., Leax, T.R. (1990) *Mater. Science and Tech.* **6**, 249.
2. Auger, P., Danoix, F., Menand, A., Bonnet, S., Bourgoin, J., Guttman, M (1990) *Mater. Science and Tech.* **6**, 301.
3. Jayet-Gendrot, S., Ould, P., Balladon, P. (1994). In : *Proceeding of Int. Symp. Fontevraud III, 12-16 Sept 1994* **1**, 90.
4. Pineau, A., Joly, P. (1991). In : *Defects assessment in components - Fundamentals and applications, ESIS/EGF9*, pp. 381-414, Mech. Engng. Publ., London.
5. Devillers-Guerville, L., Besson, J., Pineau, A (1997) *Nuclear Engng. and Design* **168**, 211.
6. Bauvineau, L.(1997) Ph.D. Thesis, Ecole des Mines de Paris, France.
7. Carassou, S., Soilleux, M., Marini, B. (1998). In : *Proceeding of Euromech-Mecamat'97, J. Phys. IV France* **8**, pp.63-70.
8. Needleman, A., Tvergaard, V. (1984) *J. of Mech. and Phys. of Solids* **32**, 461.
9. Nougier, J.P. (1987). *Méthodes de calcul numérique*. Eds. Masson, Paris.

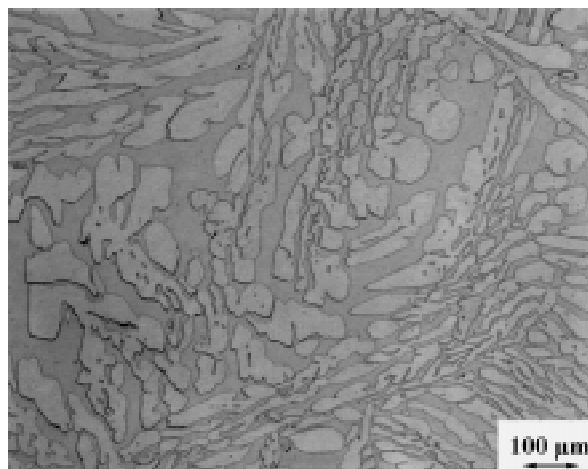


figure 1 : optical micrograph of 30% ferrite duplex stainless steel (258). Dark phase ferrite, light phase austenite.

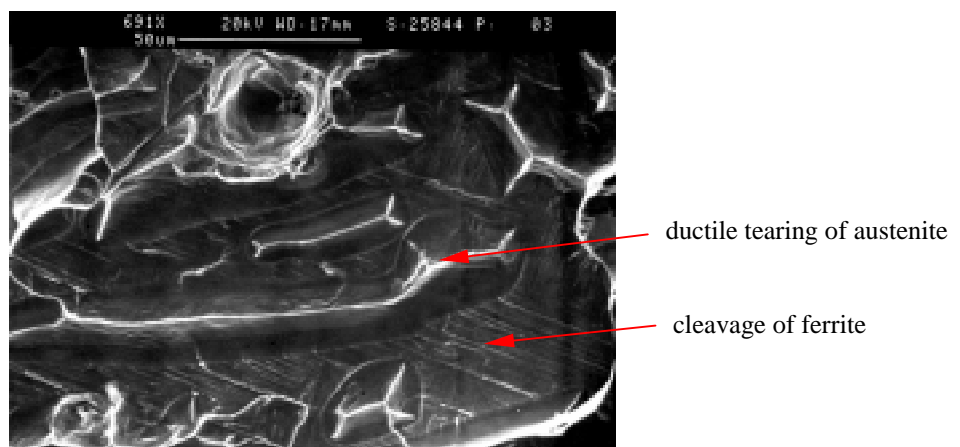


figure 2 : fractographic examination of damage mechanisms after ageing at 325°C during 30000 hours. Arrows indicate cleavage of ferrite lathes and ductile tearing of austenite.

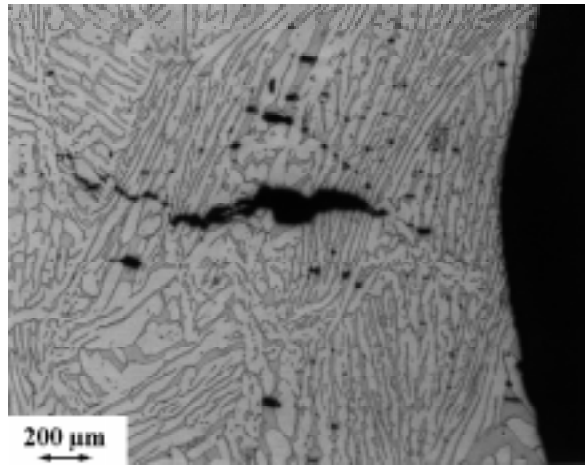


figure 3 : Macroscopic crack and cleavage cracks in steel 258 aged 30000 hours at 325°C (AE 10-6).

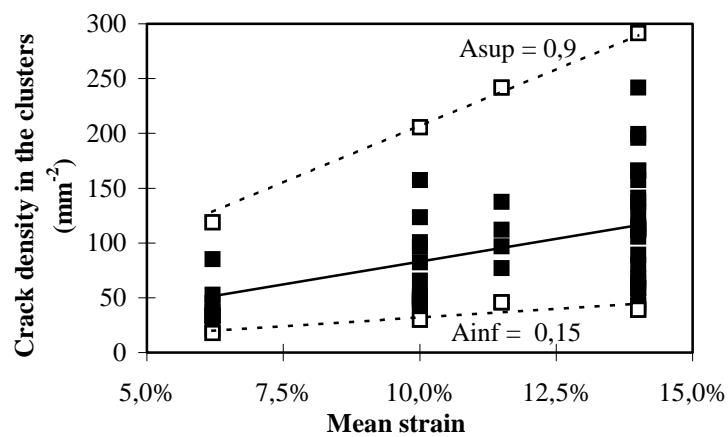


figure 4 : Experimental distribution of cleavage cracks as a function of strain (steel 258) determined from surface replicas.

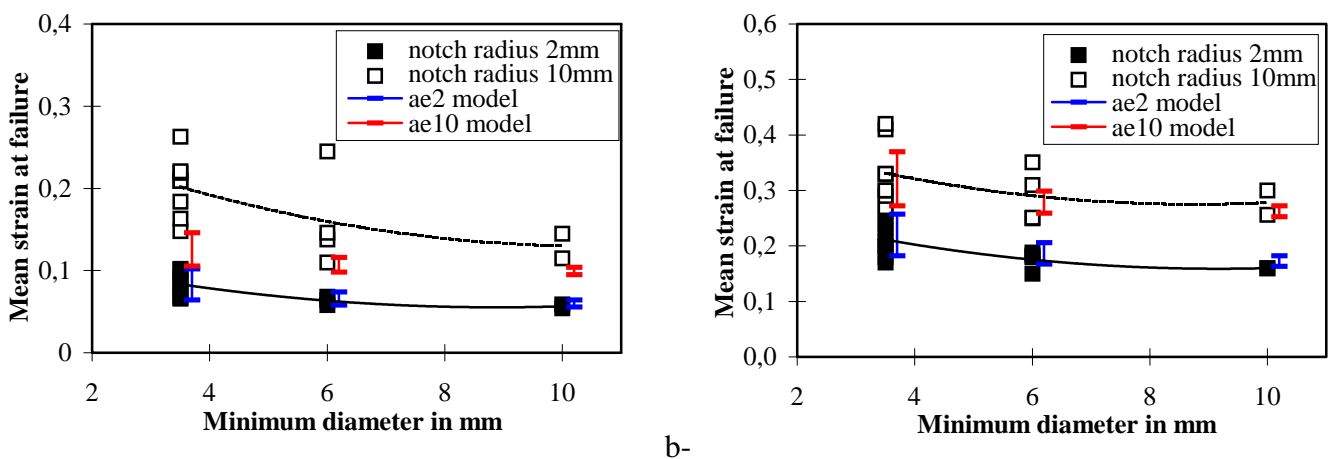


figure 5 : Experimental and simulated ductility of notched tensile specimens tested at room temperature. a- steel 258 (32% ferrite). b- steel 259 (20% ferrite)

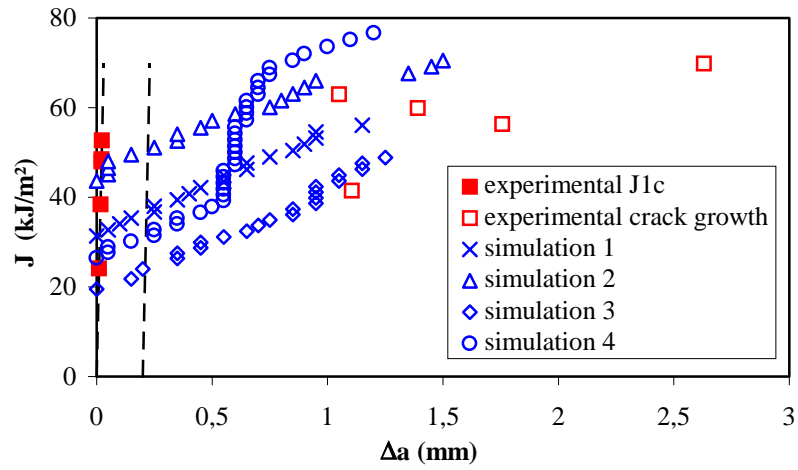


figure 6 : Experimental and simulated J- Δa plots of steel 258 tested at room temperature using 20% side groove CTJ20 specimens.

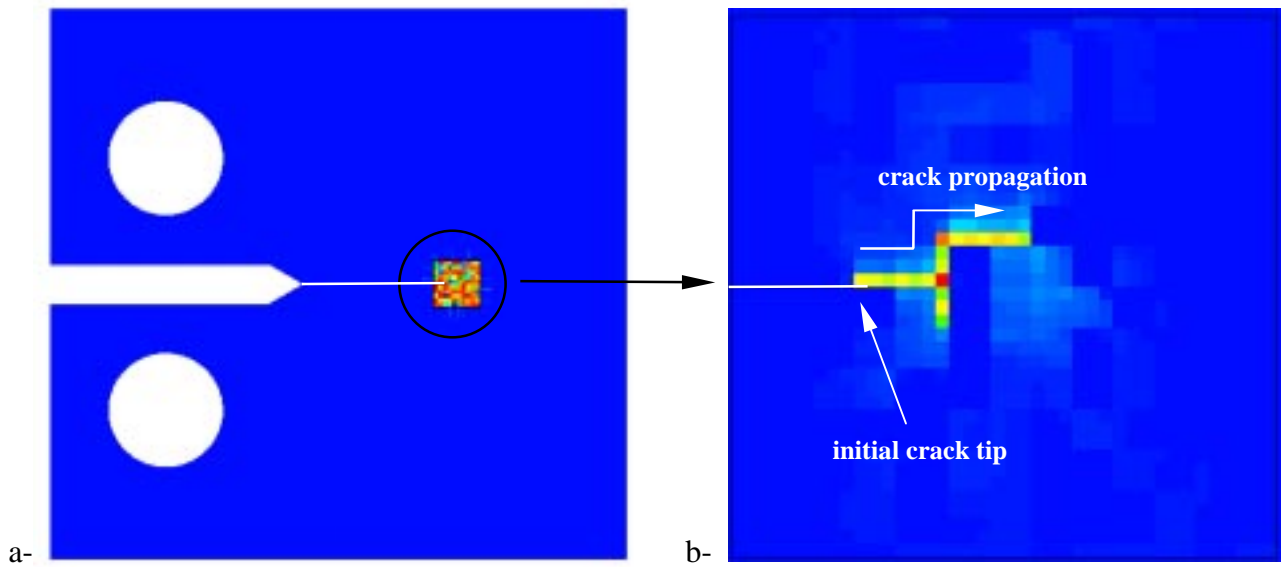


figure 7 : simulated CT specimen (simulation 4). a- distribution of nucleation rates near the crack tip. b- crack path at $\Delta a = 1.3$ mm (porosity $f_c = 7\%$ in yellow).